

AD/A-000 413

COLD CATHODE ELECTRON BEAM CONTROLLED
CO₂ LASER PERFORMANCE

Leslie L. McKee, III, et al

Air Force Weapons Laboratory
Kirtland Air Force Base, New Mexico

October 1974

DISTRIBUTED BY:

NTIS

National Technical Information Service
U. S. DEPARTMENT OF COMMERCE

This final report was prepared by the Air Force Weapons Laboratory, Kirtland Air Force Base, New Mexico, under Job Order 88091705. Captain Leslie L. McKee, III (DYS) was the Laboratory Project Officer-in-Charge.

When US Government drawings, specifications, or other data are used for any purpose other than a definitely related Government procurement operation, the Government thereby incurs no responsibility nor any obligation whatsoever, and the fact that the Government may have formulated, furnished, or in any way supplied the said drawings, specifications, or other data, is not to be regarded by implication or otherwise, as in any manner licensing the holder or any other person or corporation, or conveying any rights or permission to manufacture, use, or sell any patented invention that may in any way be related thereto.

This technical report has been reviewed and is approved for publication.

Leslie L. McKee, III
LESLIE L. MCKEE, III
Captain, USAF
Project Officer

FOR THE COMMANDER

Thomas C. May
THOMAS C. MAY
Major, USAF
Chief, X-ray Simulation Branch

David M. Ericson
DAVID M. ERICSON, JR.
Lt Colonel, USAF
Chief, Technology Division

<input type="checkbox"/> Write Section <input type="checkbox"/> Brief Section	ACCESSION FOR RTIS
	BY DISTRIBUTION/AVAILABILITY CASES
<input type="checkbox"/>	UNCLASSIFIED
<input type="checkbox"/>	NOW AVAILABLE
<input type="checkbox"/>	SPECIAL

DO NOT RETURN THIS COPY. RETAIN OR DESTROY.

ia

UNCLASSIFIED

SECURITY CLASSIFICATION OF THIS PAGE (When Data Entered)

AD/A-000 418

REPORT DOCUMENTATION PAGE		READ INSTRUCTIONS BEFORE COMPLETING FORM
1. REPORT NUMBER AFWL-TR-74-163	2. GOVT ACCESSION NO.	3. RECIPIENT'S CATALOG NUMBER
4. TITLE (and Subtitle) COLD CATHODE ELECTRON BEAM CONTROLLED CO ₂ LASER PERFORMANCE	5. TYPE OF REPORT & PERIOD COVERED Final Report 6 Jul 72 - 5 Dec 73	
	6. PERFORMING ORG. REPORT NUMBER	
7. AUTHOR(s) Capt Leslie L. McKee, Capt Steven R. Patterson, Lt Richard A. Lindstrand, and Ssgt Richard P. Kinkade	8. CONTRACT OR GRANT NUMBER(s)	
9. PERFORMING ORGANIZATION NAME AND ADDRESS Air Force Weapons Laboratory Kirtland Air Force Base, NM 87117	10. PROGRAM ELEMENT, PROJECT, TASK AREA & WORK UNIT NUMBERS Program Element 62610F Project 8809, Task 1705	
11. CONTROLLING OFFICE NAME AND ADDRESS Air Force Weapons Laboratory Kirtland Air Force Base, NM 87117	12. REPORT DATE October 1974	
	13. NUMBER OF PAGES 26 28	
14. MONITORING AGENCY NAME & ADDRESS (if different from Controlling Office) Same as block 11	15. SECURITY CLASS. (of this report) Unclassified	
	15a. DECLASSIFICATION/DOWNGRADING SCHEDULE	
16. DISTRIBUTION STATEMENT (of this Report) Approved for public release; distribution unlimited.		
17. DISTRIBUTION STATEMENT (of the abstract entered in Block 20, if different from Report) Same as block 16.		
18. SUPPLEMENTARY NOTES Reproduced by NATIONAL TECHNICAL INFORMATION SERVICE U.S. Department of Commerce Springfield VA 22151		
19. KEY WORDS (Continue on reverse side if necessary and identify by block number) Cold Cathode Electron Beam Controlled CO ₂ Laser Electron Beam CO ₂ Laser Unstable Resonator Electron Gun Mode-Locked Laser Pulse TEA Laser		
20. ABSTRACT (Continue on reverse side if necessary and identify by block number) A cold cathode electron beam controlled CO ₂ laser has been constructed. The laser has produced up to 50 joules of output energy and peak powers as high as 1 GW. Various laser system parameters which control the laser output have been investigated. The laser performance has been compared with theoretical studies.		

DD FORM 1473
1 JAN 73

EDITION OF 1 NOV 65 IS OBSOLETE

UNCLASSIFIED

SECURITY CLASSIFICATION OF THIS PAGE (When Data Entered) (28)

PREFACE

The authors would like to acknowledge the advice and constructive criticism given by Major Thomas May relating to the work described in this technical report and to the writing of it.

CONTENTS

<u>Section</u>		<u>Page</u>
I	INTRODUCTION	1
II	DESCRIPTION	6
	Electron Gun	6
	Sustainer	9
	Optical Cavity	9
	Laser Diagnostics	10
III	OPERATION	13
	Gun Duration	13
	Sustainer Bank Voltage	15
	Sustainer Bank Inductance	15
	Laser Power Output	18
	Laser Beam Characteristics	18
	Pressure Variation of Laser Output	20
IV	DISCUSSION	21
	Electron Density	21
	Electron Gun Current Through Foil	21
	Computer Calculations	23
V	CONCLUSIONS	24
	REFERENCES	26

ILLUSTRATIONS

<u>Figure</u>	<u>Page</u>
1 (a) Electron Gun Cathode Structure. (b) Closeup View of the Gun Cathode Structure Showing Details of the Gun Emitting Surface	7
2 Schematic Diagram of Electron Beam Controlled Laser	8
3 Laser Cavity	11
4 (a) Marx Generator Current, (b) Electron Gun Current, (c) Sustainer Bank Current, and (d) Laser Power Output for a Typical Shot. Horizontal scale is 300 nsec/div. Arrows indicate when the water switch crowbarred the Marx generator	12
5 (a) Peak Electron Gun Current, (b) Peak Sustainer Bank Current, (c) Total Electrical Energy into Laser Medium, and (d) Total Laser Energy Output versus Electron Gun Duration	14
6 Laser Energy Output as a Function of Sustainer Bank Voltage	16
7 Laser Output Energy versus Gun Duration for Various Sustainer Bank Inductances	17
8 Laser Output Power as a Function of Time for a 3/2/1 He/N ₂ /CO ₂ Mixture at 12.6 psi	19
9 Laser Output Power Signals Showing Mode-Locked Pulse Structure. Horizontal Sweep Rate is 50 ns/div	19
10 Laser Output Energy versus Gas Pressure for (a) Fixed 4 kV/cm Sustainer Field and (b) Fixed E/P = 3.1 kV cm ⁻¹ atm ⁻¹ .	20
11 Results of Computer Simulation of the Laser: (a) Calculated Small Signal Gain, (b) Calculated and Experimental Laser Output Power Pulses	23
12 End View of CO ₂ Laser with Both Sides On	25

SECTION I

INTRODUCTION

The uniformity of the electrical discharge in a transversely excited atmospheric pressure (TEA) CO₂ laser will be improved if the gas is first preionized prior to the occurrence of the main current pulse. One method of producing uniform ionization of the gas is through collisions with a beam of high energy electrons. Recent experiments (refs. 1 and 2) using the electron beam resulting from the thermionic emission from a hot filament (hot cathode gun) have demonstrated the ability of such a beam to stabilize large volume CO₂ laser discharges.

An alternate method for producing an electron beam which can satisfactorily control CO₂ laser discharges is from a cold cathode gun (refs. 3 and 4). The cold cathode gun can deliver much higher (~ 1 A/cm²) current densities than can the hot cathode gun. Further, the cold cathode gun is simpler in design and is particularly suited to short duration (~ 3 μ s) laser systems.

The CO₂ laser described in this report was constructed at the Air Force Weapons Laboratory (AFWL) as a cold cathode electron beam controlled laser with the above considerations in mind. The laser is to be used to form and heat target plasmas in various laser-target interaction experiments with the objective of enhancing their X-ray output.

SECTION II

DESCRIPTION

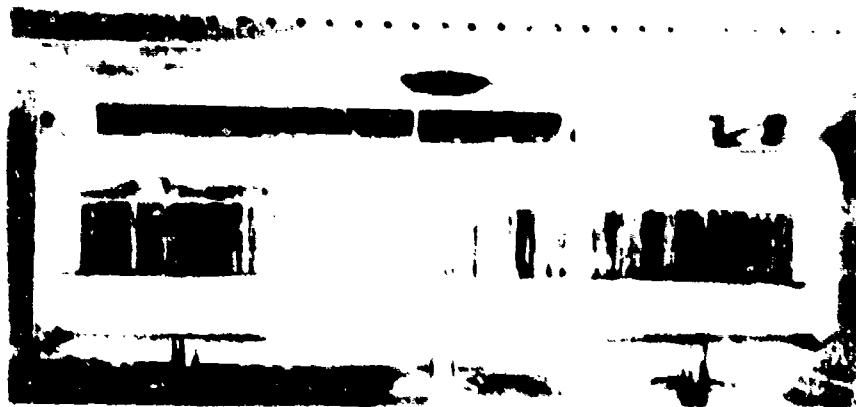
1. ELECTRON GUN

The cold cathode gun consists of a conductor which has a series of sharp edges facing the anode. The gun emits an electron beam when a rapidly rising voltage pulse is applied to the conductor. The work of Loda and DeHart (ref. 5) and of Parker (ref. 6) indicates that the high fields which result at the sharp edges cause microscopic projections, or whiskers, to grow. Field emission results from the whiskers, and the field emission current heats the whiskers and causes their vaporization. Hence, a plasma is formed along the surface of the cathode and serves as the source of the electron beam. This conducting plasma sheath is then accelerated toward the anode, and this causes the impedance of the gun to collapse when it reaches the anode by short circuiting the anode-cathode space. It has been shown (refs. 5 and 6) that prior to impedance collapse the gun can be described as a space-charge-limited diode whose spacing is decreasing at a constant rate.

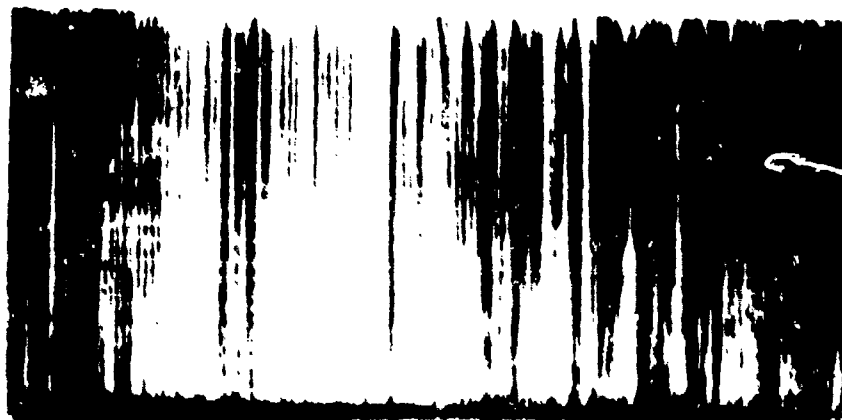
The 10 x 100 cm emitting surface of the electron gun consisted of strips of 1-mil-thick tantalum foil. The 10-cm-long strips were oriented vertical and normal to the gun cathode surface and spaced at 0.065 in intervals (16 per inch) along its 100 cm length. Figure 1 shows details of the electron gun emitting surface.

The voltage pulse for the gun was supplied by a two stage Marx generator (figure 2) which erected to 180 kV in a time of 100 ns and had an output capacitance of 0.5 μ F. The current to the gun from the Marx generator was found to be a linearly increasing ramp with a slope of about 27 kA/ μ s.

The Marx generator was triggered by a high voltage pulse delivered by a pulser unit. The pulser unit was a low inductance 26 stage Marx generator which produced a 180 kV voltage pulse with an 8 ns risetime and a 50 ns pulse width. When triggered by a thyratron, the pulser unit delivered its voltage pulse to one of the spark gaps in the electron gun Marx generator (figure 2). This command trigger unit caused the Marx to erect with a jitter time of about 23 ns. The jitter time for the laser output pulse was about 48 ns.



(a)



(b)

Figure 1. (a) Electron Gun Cathode Structure. (b) Closeup View of the Gun Cathode Structure Showing Details of the Gun Emitting Surface.

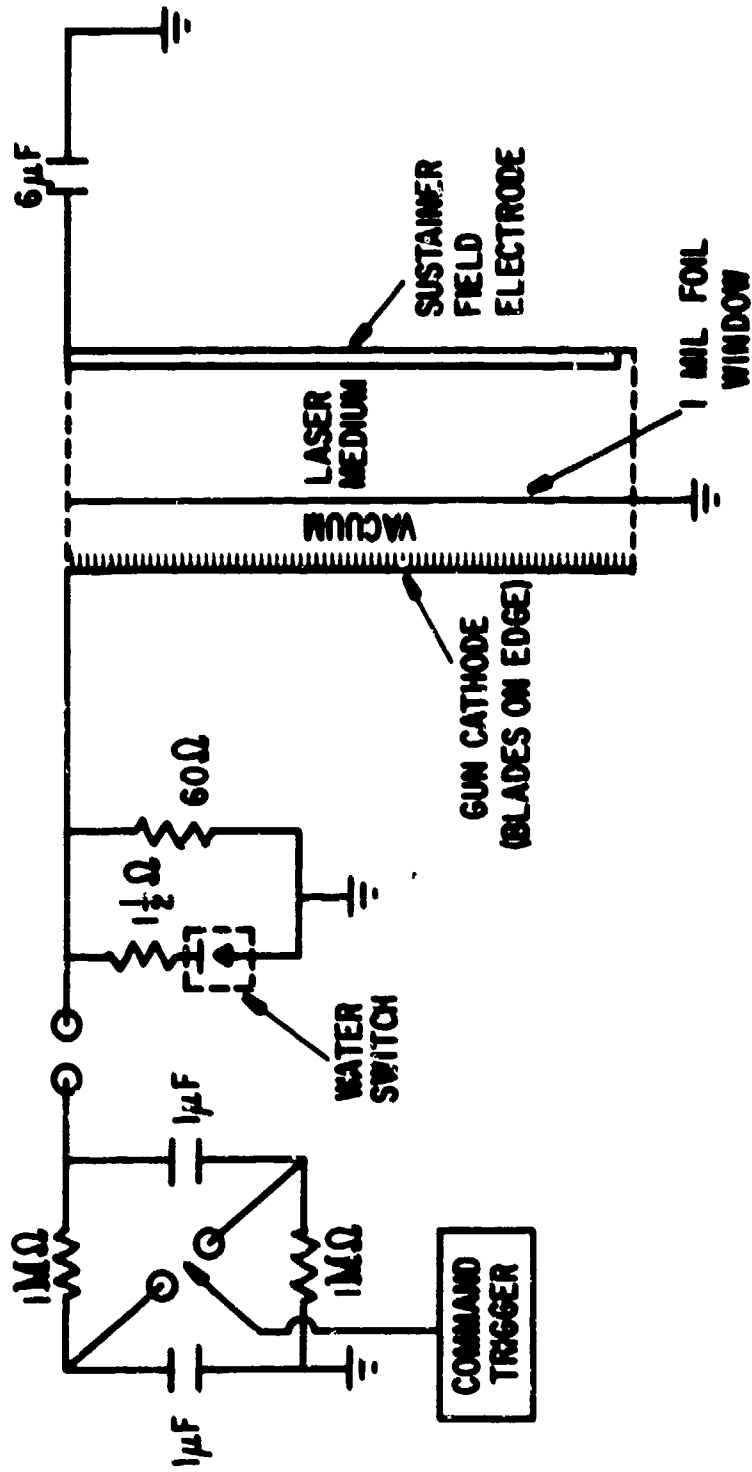


Figure 2. Schematic Diagram of Electron Beam Controlled Laser.

The gun cathode structure was located in an evacuated chamber (figure 1a, sides removed). Typical operating pressures were about 2×10^{-5} Torr to 1×10^{-4} Torr. The evacuated chamber was separated from the laser cavity by a 10x100 cm 1-mil-thick titanium foil which maintained the vacuum while transmitting the electron beam. The anode for the gun was a grounded 10x100 cm aluminum screen located on the gun side of the foil. The separation between the gun and the grounded screen was 4 cm.

As mentioned previously, the impedance of the gun collapses when the plasma sheath formed at the cathode surface reaches the anode. The cathode-anode arc which will result can damage the foil and cause it to lose its vacuum seal. To prevent this, it is necessary to crowbar the Marx generator before impedance collapse so that its full voltage is no longer applied to the gun. This was done with a water switch (figure 2).

The water switch is a positive point-negative plane water spark gap. It has been shown that the streamer velocity in water for such a spark gap is constant (ref. 5). Hence, the propagation time of the streamer was linearly dependent on the gap spacing. Thus, the duration of the gun current could be varied by changing the gap spacing of the water switch. The range of gun durations used was about 300 ns to 1.5 μ s.

2. SUSTAINER

The main discharge in the laser medium was driven by a 6 μ F, 40 kV sustainer capacitor bank (figure 2). During normal operation of the laser, the sustainer bank was charged to apply a DC electric field prior to the firing of the electron gun. When the gun was fired, the resulting electron beam ionized the laser medium, and the sustainer-driven discharge followed. The peak current of the sustainer discharge occurred when the water switch crowbarred the electron gun Marx generator and was typically about 70 kA.

3. OPTICAL CAVITY

The gas mixture used for the laser medium was contained in a plexiglass box measuring 100x10x35 cm internally or 35 liters in volume. The volume in which lasing occurred was a cylinder 10 cm in diameter and 100 cm in length or 7.85 liters in volume.

The gas mixture used for lasing consisted of variable proportions of carbon dioxide, nitrogen, and helium. The gas mixture was flowed through the box by admitting it at one end and venting it to the atmosphere at the other. This was

done to prevent the gas from heating after successive shots, since the laser gain decreases with temperature due to thermal population of the lower laser levels. The gas mixture was pressurized to 0.2 to 5.0 psi above local atmospheric pressure (12.2 psi) by adjustment of the venting valve.

The cavity optics are shown in figure 3. The laser was operated as an unstable resonator with a 10 m radius of curvature, 12.7-cm-diameter concave mirror at one end and a 5 m radius of curvature, 5-cm-diameter convex mirror at the other. Following Siegman (ref. 7), the cavity parameters are $g_1 = 3/2$, $g_2 = 3/4$ so that the cavity will be confocal when the mirror separation is 2.5 m. The laser output was coupled out of the cavity by an output coupler of the type used by Krupke and Sooy (ref. 8). The output coupler was a flat, 15-cm-diameter mirror with a 4.5-cm-diameter hole drilled through its center at an angle of 45 degrees. Using geometric optics, this oscillator cavity had an output coupling of 79 percent. When diffraction effects are considered (ref. 7), the output coupling should be 56 percent.

The laser beam diameter was determined by the 10-cm-diameter output aperture of the plexiglass box. The gas mixture in the box was contained by a 1-1/2 inch-thick flat piece of NaCl covering the output aperture.

4. LASER DIAGNOSTICS

The current in the ground line of the electron gun Marx generator was monitored by a 0.001-ohm current viewing resistor. A typical signal from this resistor is shown in figure 4a. The current to the electron gun from the Marx generator was monitored by a Rogowski coil on the cable to the gun. The gun current corresponding to figure 4a is shown in figure 4b. The sustainer current was measured with another Rogowski coil. Figure 4c shows the sustainer current for the conditions of figures 4a and 4b.

The optical output of the laser was detected by means of a photon drag detector and a thermopile. One flat piece of NaCl was used as a beam splitter to reflect 8 percent of the beam onto the photon drag detector, while another flat piece of NaCl reflected an additional 8 percent portion of the beam onto the thermopile (so that about 85 percent of the laser output energy could be delivered to a target). The photon drag detector was used to monitor the laser power output and had a response time of about one nanosecond. A typical photon drag signal is shown in figure 4d. The thermopile was used to measure laser energy. Typical laser energies were in the range of 10 to 40 joules.

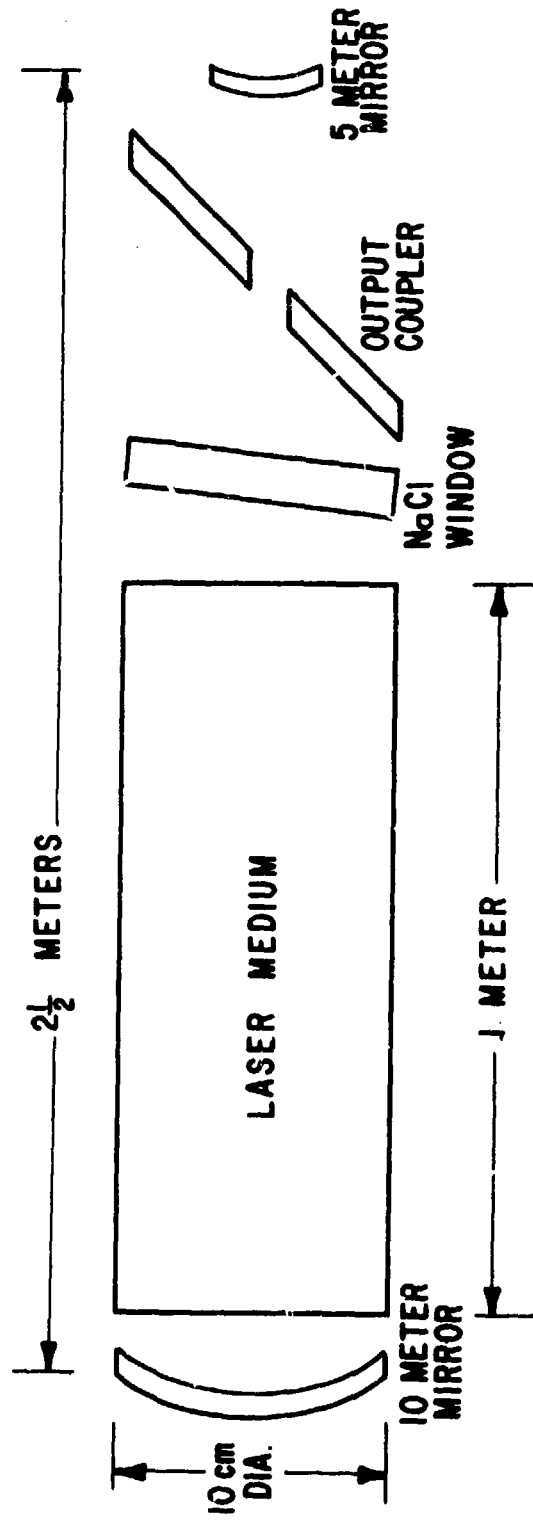


Figure 3. Laser Cavity.

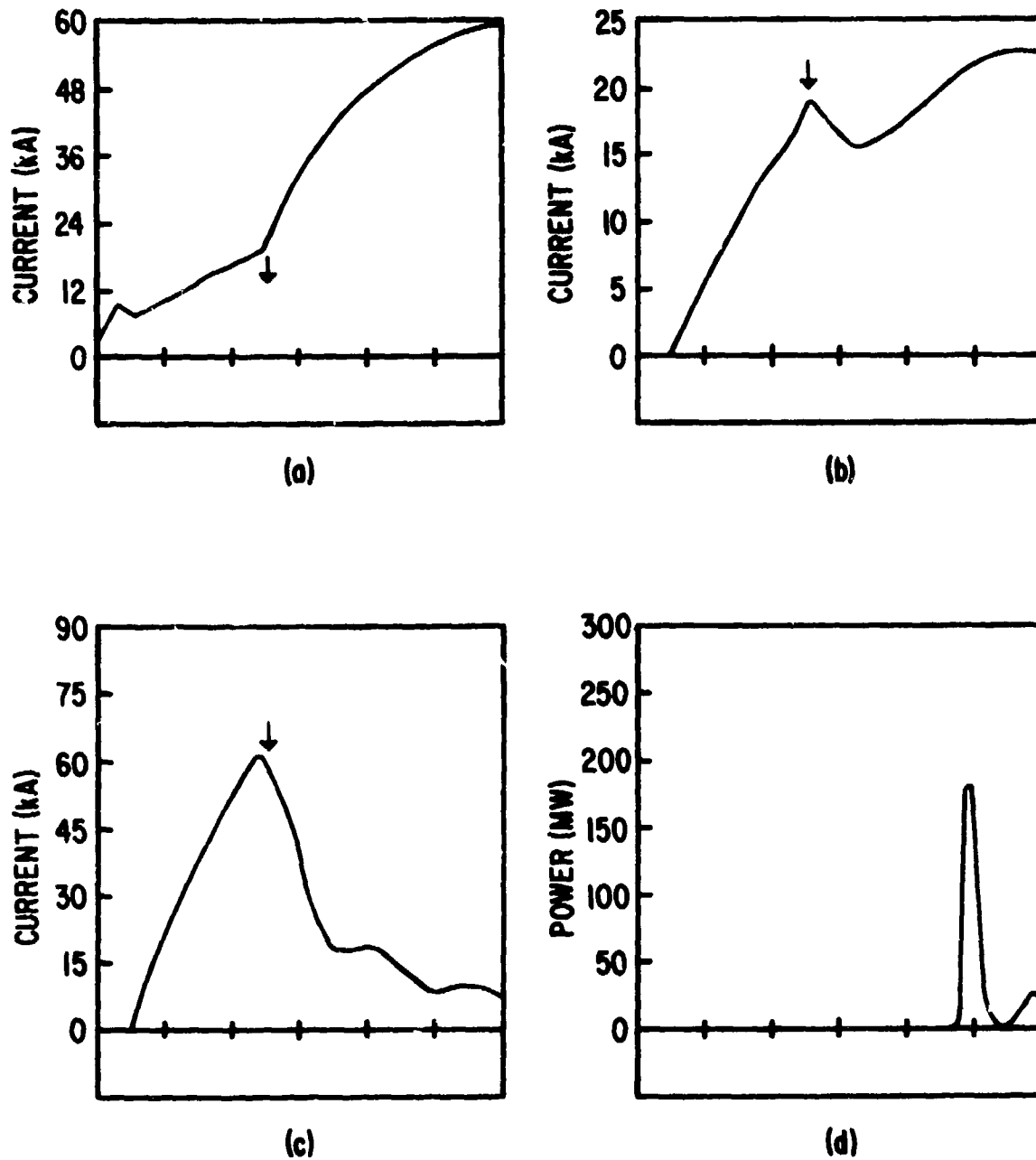


Figure 4. (a) Marx Generator Current, (b) Electron Gun Current, (c) Sustainer Bank Current, and (d) Laser Power Output for a Typical Shot. Horizontal scale is 300 nsec/div. Arrows indicate when the water switch crowbarred the Marx generator.

SECTION III OPERATION

1. GUN DURATION

As figure 4b shows, the current to the electron gun increased approximately linearly with time until the Marx generator was crowbarred, at which time the gun current remained more or less constant for several microseconds. The time period of the linear increase of the gun current is defined as the "gun duration." For example, in figure 4b the gun duration is about 600 ns.

The gun duration is an important parameter for characterizing the performance of the laser. The manner in which the gun duration governed the peak electron gun current, the peak sustainer bank current, the total electrical energy into the laser medium, and the total laser energy output is illustrated in figure 5. The values indicated in this figure were obtained for a sustainer bank voltage of 40 kV, a CO₂/N₂/He mixture in the ratio 1/2.4/3.9, and a gas pressure of 1.6 psi above local atmospheric pressure (12.2 psi).

Figures 5a and 5b show that both the electron gun current and the sustainer bank current increased approximately linearly with time prior to the crowbarring of the Marx generator. The slope of figure 5a shows that the average rate of increase of the gun current was about 24 kA/ μ s before crowbarring.

Figure 5c indicates how the electrical energy input into the laser medium from the sustainer capacitor bank increased with the gun duration. This energy input was the result of the dissipation of the sustainer current in the laser medium and was calculated from the voltage drop on the sustainer capacitor bank after the laser was fired. For example, an energy input of 1600 joules corresponded to a drop of about 8 kV in the sustainer voltage for a sustainer bank capacitance of 5.55 μ F. The sustainer bank stored 4440 joules initially at 40 kV.

Figure 5d shows that the laser energy output also increased with gun duration, as would be expected. Comparing figures 5c and 5d reveals that between 1.5 percent and 3.2 percent of the electrical energy into the laser medium was converted into energy in the laser pulse.

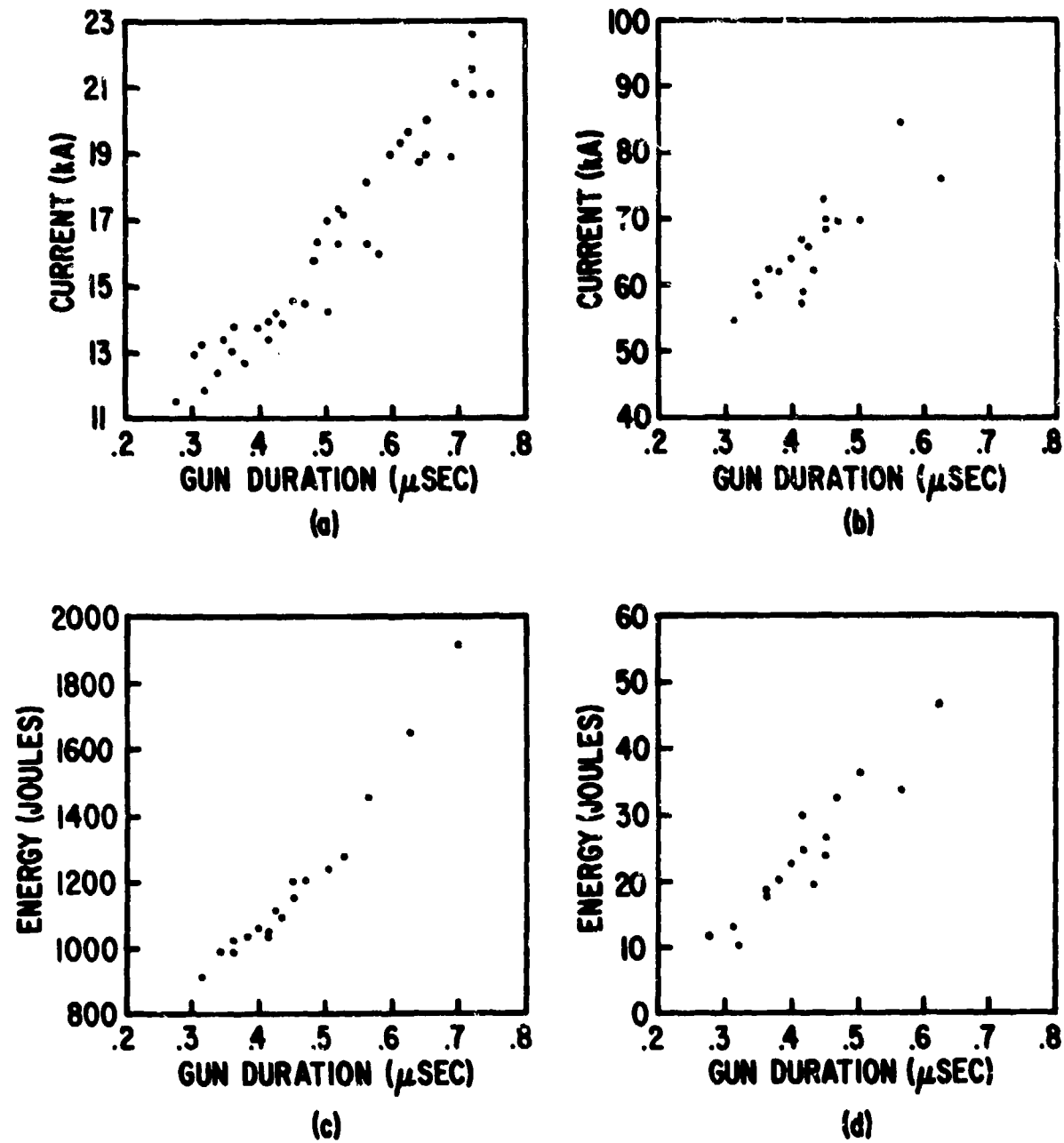


Figure 5. (a) Peak Electron Gun Current, (b) Peak Sustainer Bank Current, (c) Total Electrical Energy into Laser Medium, and (d) Total Laser Energy Output versus Electron Gun Duration.

The increase of laser energy output with gun duration illustrated in figure 5d did not continue for very long gun durations. Instead, the laser energy output was found to decrease with gun duration for durations longer than about one microsecond. Also, the foil between the electron gun and the lasing medium may be damaged when the gun duration is so long. The optimum gun duration was found to be between 600 ns and 800 ns.

2. SUSTAINER BANK VOLTAGE

The sustainer bank voltage could also be varied. The manner in which varying this voltage affected the laser energy output is illustrated in figure 6. The laser medium gas mixture and pressure were the same as for the data in figure 5. The spread in the data points at each voltage value was caused primarily by the fact that the gun duration was not the same for each shot.

Figure 6 indicates that the laser output increased with sustainer bank voltage. This is to be expected since both the sustainer current and the electrical energy input increased with sustainer bank voltage. The practical limit for the sustainer voltage was 42 kV. Since this voltage was applied as a DC field before the laser was fired, a higher voltage would result in air breakdown and arcing before lasing could occur.

3. SUSTAINER BANK INDUCTANCE

Three sustainer bank capacitor configurations were used in the course of this investigation. First used was a 5.55 μF bank consisting of three 1.85 μF capacitors in parallel. This bank was used to obtain the data presented in figures 4, 5, and 6 and had an inductance of about 150 nH. Next, two of these capacitors were connected in parallel to give a 3.7 μF bank with an inductance of about 225 nH. Also used was a sustainer bank constructed of three 2 μF capacitors in parallel. This third bank used a low inductance transmission plate to connect the capacitors to the sustainer anode, giving an inductance of only 57 nH.

There were notable differences between the data obtained with these three banks. Figure 7 shows that the two higher inductance banks gave higher laser output energies than did the lowest inductance bank. The reason for these differences is not entirely clear from this investigation. Gain measurements using each of the three sustainer bank configurations will be required to resolve these differences.

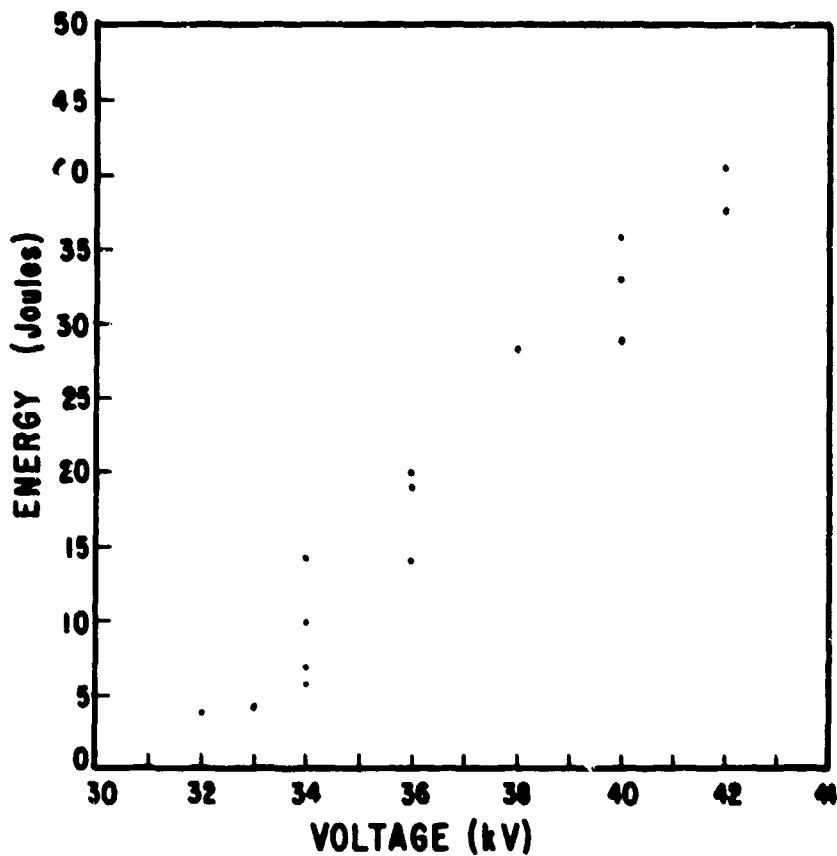


Figure 6. Laser Energy Output as a Function of Sustainer Bank Voltage.

4. LASER POWER OUTPUT

The laser power output appeared as a gain switched spike with a typical half-width of 80 ns followed by a lower power hump and tail with a duration of 1 to 2 μ s. A typical laser power output pulse is illustrated in figure 8.

Typically, the laser output energy was about equally divided between the gain switched spike and the tail. The actual distribution of energy between these two parts of the laser power signal varied from shot to shot, depending primarily on the laser medium gas mixture and pressure.

The magnitude of the laser power output depended quite sensitively on the optical alignment of the laser cavity. In general, the better the alignment was, the higher the peak laser power was. The highest laser output power measured was 577 MW. This power corresponded to a total laser output energy of 40.4 joules and a gain switched spike pulse width of 35 ns obtained with a 4/2.4/1 He/N₂/CO₂ mixture at 13.7-psi pressure.

As figure 9 shows, the laser power signal actually consisted of a train of mode-locked pulses whose amplitude envelope was the general pulse shape of figure 8. The spacing of the mode-locked pulses was about 15 ns which corresponded to the cavity round trip time, $2L/c$ ($L = 2.5$ m). The photon drag detector was unable to resolve the width of each mode-locked pulse. However, the theoretically predicted pulse width for mode-locked pulses from this laser would be about 1 ns (ref. 9). As a result, the peak powers of the mode-locked pulses were enhanced by an order of magnitude above the peak power estimated for the nonmode-locked pulse shape of figure 8, so that peak powers of several gigawatts actually resulted. The uniformity of the mode-locking across the laser beam was checked. It was found that the mode-locked pulses had the same structure at different points across the laser beam. Hence, the laser pulse retained its mode-locked structure when focussed down.

5. LASER BEAM CHARACTERISTICS

Due to the nature of the laser cavity output coupler (figure 3), the laser beam emerging directly from the laser was annular, i.e., there was zero laser intensity along its propagation axis. The distribution of laser energy in the beam was studied by examining the burn pattern that the beam made when it irradiated burn paper. Most of the laser energy was found to be concentrated in an annulus with an outer diameter of 7.3 cm and an inner diameter of 5.3 cm.

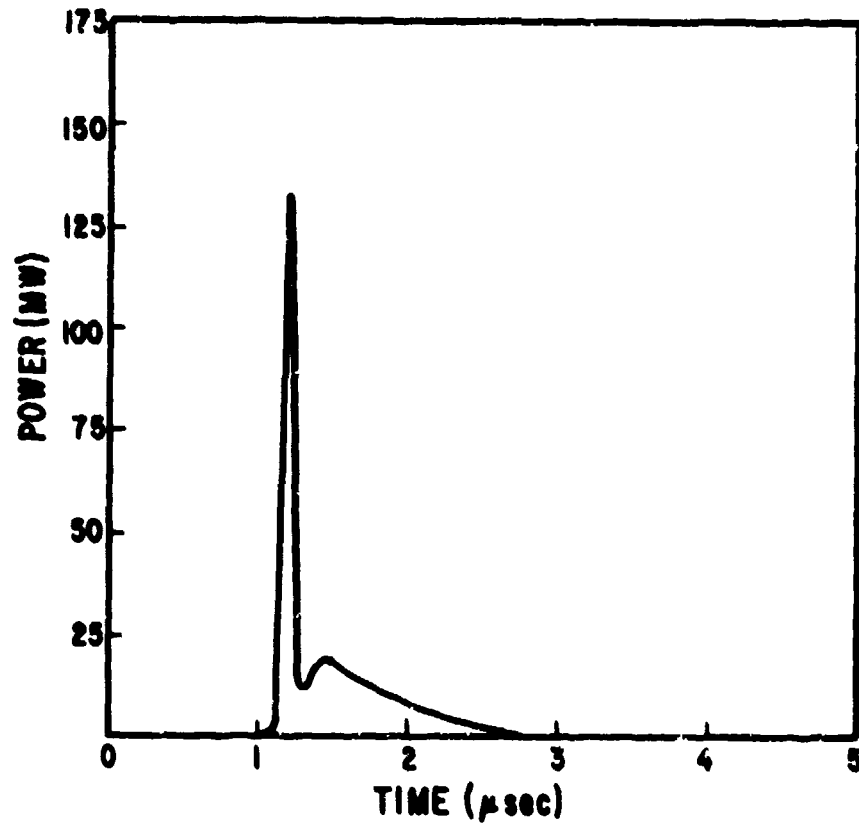


Figure 8. Laser Output Power as a Function of Time for a 3/2/1 He/N₂/CO₂ Mixture at 12.6 psi.

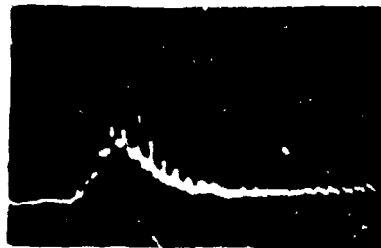


Figure 9. Laser Output Power Signals Showing Mode-Locked Pulse Structure. Horizontal Sweep Rate is 50 ns/div.

Thus, the maximum energy and power densities of the laser output beam were about 25 J/cm² and 300 MW/cm² for the mode-locked spikes.

The divergence of the laser beam was determined rather crudely by taking and comparing burn patterns at two different distances separated by about one meter. This test indicated that the full angle beam divergence was about 4 mrad. It should be emphasized here that this value was crudely determined. The beam divergence needs to be remeasured using a more accurate method.

6. PRESSURE VARIATION OF LASER OUTPUT

The variation of the laser output with the pressure of the laser medium was investigated. In the first test the pressure was increased while the sustainer voltage was held constant at 40 kV (using the 57 nH bank). The results are given in figure 10a which shows that the laser output energy decreased with increasing pressure.

In the second test the pressure was increased while the ratio of the sustainer electric field to the pressure (E/P) was held fixed at about 3.1 kV cm⁻¹ atm⁻¹. Figure 10b shows that in this case the energy tended to increase with pressure. The data are compatible with an increase in energy of 50 percent as the pressure increased from 12 psi to 18 psi. That rate of increase was computed theoretically by a computer code written by Captain Hugh Southall of AFWL (ref. 11) and is indicated in figure 10b as the dashed line.

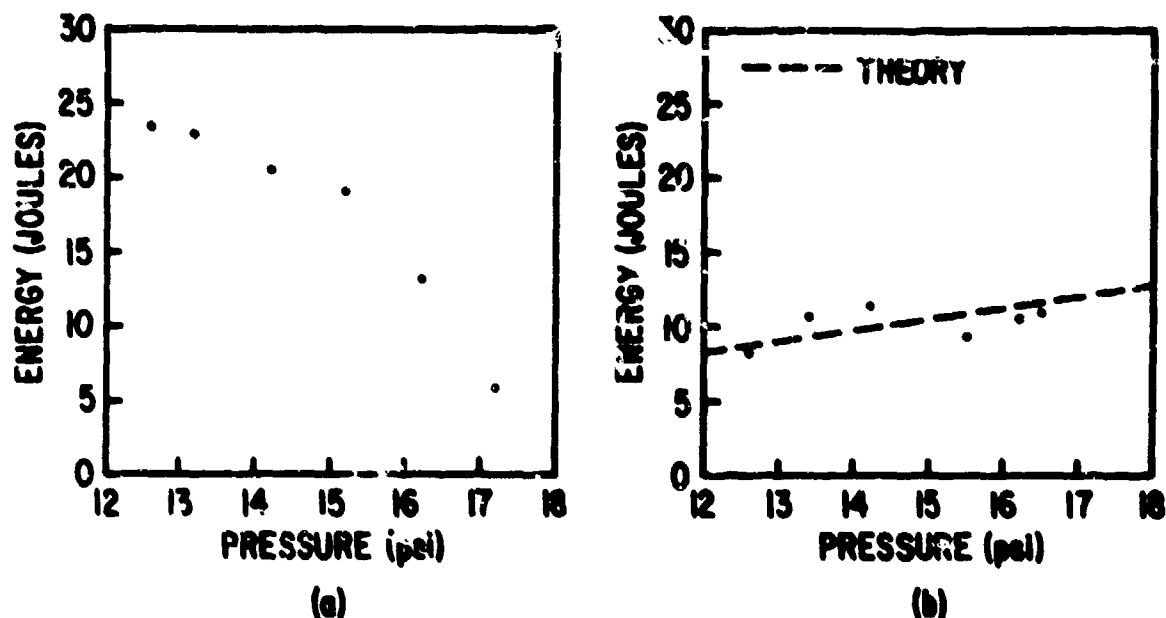


Figure 10. Laser Output Energy versus Gas Pressure for (a) Fixed 4 kV/cm Sustainer Field and (b) Fixed E/P = 3.1 kV cm⁻¹ atm⁻¹.

SECTION IV
DISCUSSION

1. ELECTRON DENSITY

The electron density of the lasing medium can be estimated by applying

$$j = n_e e v_d \quad (1)$$

where j is the sustainer bank current density, n_e is the electron density, e is the electronic charge, and v_d is the drift velocity of the electrons in the sustainer field. Estimate j by dividing the sustainer current by the cross-sectional area of the active laser volume (1000 cm^2). Estimate v_d from published calculations (ref. 10) giving v_d as a function of E/n for a given laser gas mixture.

Typical experimental conditions were $E/n = 1.16 \times 10^{-16} \text{ volt-cm}^2$ and j at electron gun cut-off was about 59.3 A/cm^2 . This gives a drift velocity of $v_d = 4.0 \times 10^6 \text{ cm/sec}$ and an electron density of $n_e = 9.3 \times 10^{13} \text{ cm}^{-3}$ at electron gun cut-off.

2. ELECTRON GUN CURRENT THROUGH FOIL

The electron gun current density after passing through the foil was significantly lower than the current delivered to the electron gun from the Marx generator. The difference is due to the absorption and scattering of the electron beam as it passes through the foil and the foil support structure. An estimate of the transmitted electron gun current density can be obtained by using the equation which governs the electron density in the laser gun medium:

$$\frac{\partial n_e}{\partial t} = S - \alpha_r n_e^2 \quad (2)$$

where α_r ($\approx 10^{-7} \text{ cm}^3/\text{sec}$) is the average recombination coefficient and S is the source term given by

$$S = \frac{J_{eb} \beta}{e} \quad (3)$$

J_{eb} is the electron beam current density (primary electrons) after passing through the foil and β ($\approx 136/\text{cm}$) is the average number of ion pairs created per

centimeter by a primary electron. The steady state electron density which is attained in a time of $(25\alpha_r)^{-1}$ seconds is given by

$$n_{ss} = (S/\alpha_r)^{1/2} \quad (4)$$

Using the electron density determined in the above example, $n_{ss} = 9.3 \times 10^{13} \text{ cm}^{-3}$, the source term becomes $S = 8.6 \times 10^{20} \text{ cm}^{-3} \text{ sec}^{-1}$ from equation 4. Then according to equation 3 J_{eb} is roughly 1.0 A/cm^2 at electron gun cut-off. The current from the Marx generator at that time was 14.0 A/cm^2 . Hence, this crude analysis indicates that the electron beam was attenuated by about an order of magnitude in passing through the foil.

3. GAIN

As of yet, gain measurements have not been performed for the CO_2 laser. However, it is possible to estimate the gain from the delay in the appearance of the laser output power pulse.

The equation for the growth of the laser power intensity with time is

$$\frac{dI}{dt} = c \frac{dI}{dz} = (g - g_c) c I \quad (5)$$

where g is the gain and g_c is the threshold or cavity gain. The solution of equation 5 is

$$I = I_0 e^{(g - g_c) c t} \quad (6)$$

Hence, the characteristic growth time of the laser intensity is

$$\tau = \frac{1}{(g - g_c) c} \quad (7)$$

The cavity gain is given by

$$g_c = - \frac{1}{2L} \ln[R_1(R_2 - K)(1 - \alpha)] \quad (8)$$

where L is the cavity length, R_1 and R_2 are the reflectivities of the back and front mirrors respectively, K is the output coupling fraction, and α is the absorption loss of the NaCl window (figure 3). Using $R_1 = 0.9$, $R_2 = 0.9$, $K = 0.6$, and $\alpha = 0.2$, equation 8 gives $g_c = 0.77 \text{ percent cm}^{-1}$.

An estimate of the gain can be made by finding the value of the gain which gives the observed delay in the occurrence of the laser power output pulse. For the purpose of this estimate, the gain is assumed to increase linearly with time

from the beginning of the electron gun current until its cut-off. After cut-off, the gain is assumed to remain constant until the laser output power has grown to about 10 percent of its observed maximum. I_0 in equation 6 is taken to be the power level of the spontaneous emission background noise from which the laser oscillations grow ($\approx 10^{-28}$ watt/cm²). For a gun duration of 760 nsec and $E/n = 1.16 \times 10^{-16}$ volt cm², the gain which gives the proper lasing delay (510 ns after electron gun cut-off) is about 1.2 percent cm⁻¹.

4. COMPUTER CALCULATIONS

The behavior of an electron beam controlled CO₂ laser was modelled by a computer code written by Hugh Southall of AFWL (ref. 11). This program uses the electron gun and sustainer currents for the laser to predict the laser's output. The program also computes the small signal gain.

Figure 11 shows the computed small signal gain and laser output power pulse. The experimental conditions were a gun duration of 760 ns (gun cuts off at 960 ns in figure 11), a peak sustainer current of about 56 kA, an average sustainer field of 3.3 kV/cm, a gas mixture of 4/2.4/1 of He/N₂/CO₂, and a gas pressure of 13.7 psi. As figure 11a shows, a peak small signal gain of about 1.6 percent cm⁻¹ was predicted by the computer program. However, figure 11b shows that the predicted laser power pulse occurred much earlier and was larger in magnitude than the observed pulse. This indicates that the small signal gain was less than that predicted. The actual value of the gain probably lies between 1.2 percent cm⁻¹ (as estimated in section III above) and 1.6 percent cm⁻¹.

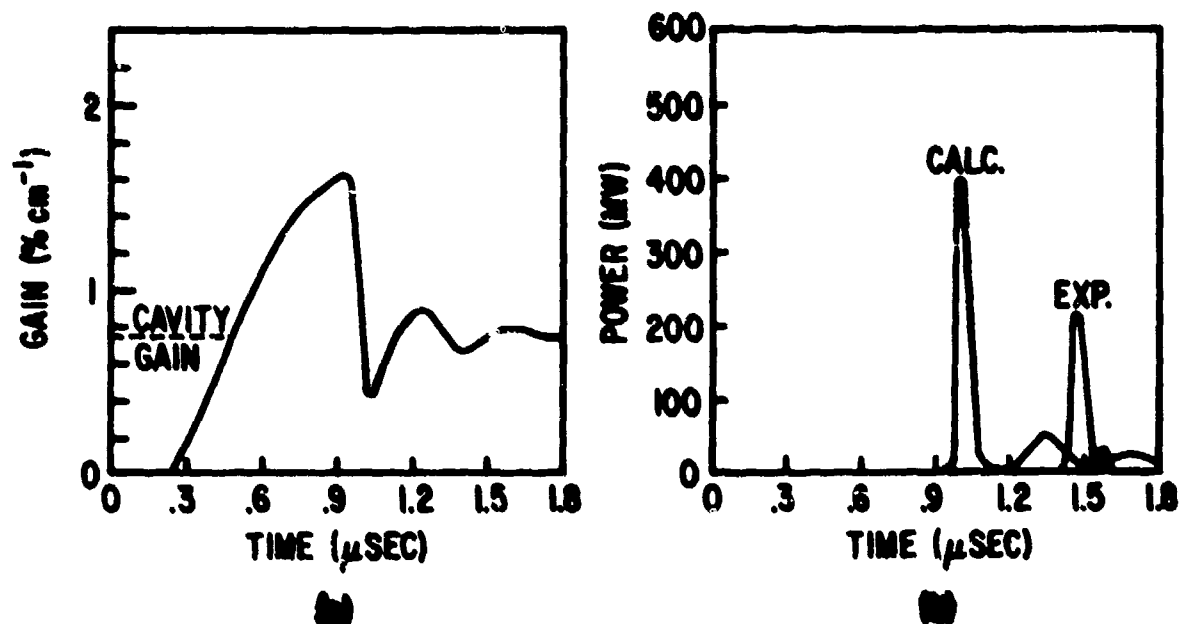


Figure 11. Results of Computer Simulation of the Laser: (a) Calculated Small Signal Gain, (b) Calculated and Experimental Laser Output Power Pulses.

SECTION V
CONCLUSIONS

The electron gun structure has been designed and constructed so that an electron beam can be produced on both sides of it. When gun blade structures are put on both sides, then the gun can control discharges on both sides simultaneously. Figure 12 shows the configuration.

With both sides on, it will be possible to operate one side as an oscillator and the other as an amplifier by directing the output from one side (oscillator) through the other (amplifier). Also both sides can be operated as amplifiers to amplify a beam provided by another oscillator CO₂ laser. Amplification can then be obtained either by running the oscillator beam first through one side and then the other or by splitting the oscillator beam into two parts and running each part through a side simultaneously and then recombining the two amplified beams.

The output of the laser can also be increased by increasing the sustainer field voltage and by pressurizing the laser medium to 2 to 3 atmospheres. These methods of increasing the output of the laser are to be put into practice in the near future at the Air Force Weapons Laboratory.

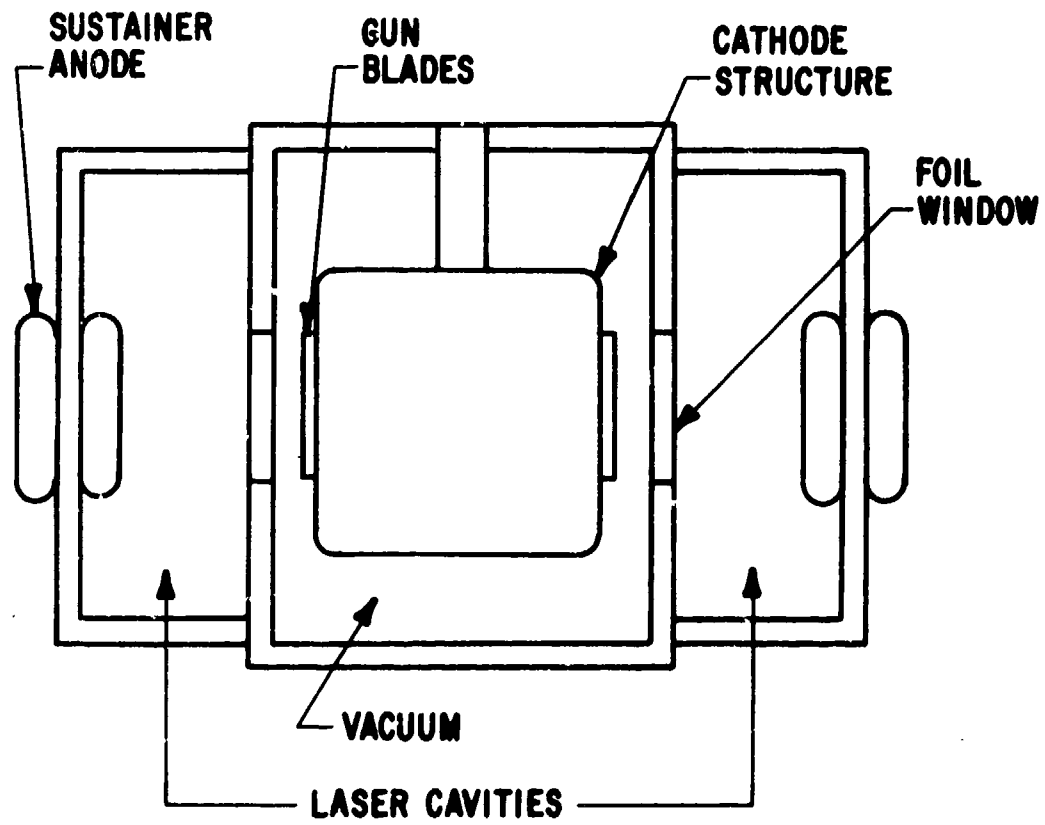


Figure 12. End View of CO₂ Laser with Both Sides Attac'ed.

REFERENCES

1. C. A. Fenstermacher, M. J. Nutter, W. T. Leland, and K. Boyer, Appl. Phys. Lett. 20, 56, 1972.
2. J. D. Daugherty, E. R. Pugh, and D. H. Douglas-Hamilton, Bull. Am. Phys. Soc. 17, 399, 1972.
3. H. G. Ahlstrom, et al., Appl. Phys. Lett. 21, 492, 1972.
4. C. Cason, G. J. Dezenberg, and R. J. Huff, Appl. Phys. Lett. 23, 110, 1973.
5. G. Loda and T. DeHart, Physics International Report No. PIFR-326 (unpublished).
6. R. K. Parker, Explosive Electron Emission and the Characteristics of High-Current Electron Flow, Ph. D. Thesis, University of New Mexico, 1973 (unpublished).
7. A. E. Siegman, Laser Focus 7, 42, 1971.
8. W. F. Krupke and W. R. Sooy, IEEE Journal Quant. Elec. QE-5, 575, 1969.
9. O. R. Wood, et al., Appl. Phys. Lett. 17, 376, 1970.
10. W. L. Nighan, Phys. Rev. 2, A1989, 1970.
11. H. L. Southall, W. A. Proctor, and G. H. Canavan, "Prediction of Small Signal Gain for a Pulsed E-Beam CO₂ Laser," Laser Digest, Fall 1972, p. 155.